Published in final edited form as:
Mol Pharm. 2013 November 4; 10(11): 4099–4106. doi:10.1021/mp4005468.

In vivo safety evaluation of polyarginine coated magnetic nanovectors

Omid Veiseh[a,b], **Forrest M. Kievit**[b], **Vicki Liu**[c], **Chen Fang**[d], **Zachary R. Stephen**[a], **Richard G. Ellenbogen**[b], and **Miqin Zhang**[a,b,*]

[a]Department of Materials Science and Engineering, University of Washington, Seattle, Washington 98195

[b]Department of Neurological Surgery, University of Washington, Seattle, Washington 98195

[c]Department of Bioengineering, University of Washington, Seattle, Washington 98195

[d]Fred Hutchinson Cancer Research Center, Seattle, Washington 98195

Abstract

Safety and efficacy are of critical importance to any nanomaterial-based diagnostic and therapy. The innocuity and functionality of a nanomaterial in vivo is largely dependent on the physicochemical properties of the material, particularly its surface coating. Here, we evaluated the influence of polycationic coating on the efficacy, clearance organ uptake, and safety of magnetic nanovectors designed for siRNA delivery. Polyethylene glycol (PEG) coated superparamagnetic iron oxide nanoparticles (NPs) of 12 nm in core diameter were modified with a polycationic coating of either poly-L-arginine (pArg) or polyethylenimine (PEI) and further covalently functionalized with siRNA oligonucleotides. The produced NP-pArg-siRNA and NP-PEI-siRNA nanovectors were similar in hydrodynamic size (21 nm and 22 nm, respectively), but significantly differed in zeta potentials (+2.1 mV and +29.8 mV, respectively). Fluorescence quantification assays revealed that the NP-pArg-siRNA nanovector was 3-fold more potent than NP-PEI-siRNA in delivering siRNA, and 1.8-fold more effective in gene silencing when tested in rat C6 glioblastoma cells. In vivo, both nanovector formulations were similarly taken up by the spleen and liver as determined by histopathological and hemopathological assays. However, PEI coated nanovectors elicited severe hemoincompatibility and damage to the liver and spleen while pArg coated nanovectors were found to be safe and tolerable. Combined, our findings suggest that polycationic coatings of pArg were more effective and safer than commonly used PEI coatings for preparation of nanovectors. The NP-pArg-siRNA nanovector formulation developed here shows great potential for in vivo based biomedical applications.

Keywords

iron oxide nanoparticle; gene therapy; cancer; nanotechnology; siRNA

INTRODUCTION

RNA interference (RNAi) is an intrinsic biological pathway through which cells can regulate gene expression.[1] The RNAi pathway can be exploited for the treatment of many

*Corresponding author: Miqin Zhang, Department of Materials Science and Engineering, University of Washington, 302L Roberts Hall, Box 352120, Seattle, WA 98195, USA. Telephone: 206-616-9356; Fax: 206-543-3100; mzhang@u.washington.edu.

SUPPORTING INFORMATION AVAILABLE

Quantitative analysis for degree of hemolysis. This information is available free of charge via the Internet at http://pubs.acs.org/.

debilitating diseases where aberrant gene expression contributes to its pathogenesis, such as cancer.[2] Successful in vivo delivery of small interfering RNA (siRNA) to diseased cells in the body remains a major impediment to the clinical application of RNAi based therapeutics.[3] One emerging technology aimed at addressing this challenge are nanomaterial-based non-viral vectors (nanoparticles) as carriers for delivery of siRNA.[4] For such applications, the development of superparamagnetic iron oxide nanoparticles (SPIONs) as nanovectors is of particular interest because of their safe toxicity profile and magnetic property that can be exploited for in vivo magnetic resonance imaging (MRI).[5, 6] Critical to the success of magnetic nanovectors is the apt design and integration of coatings to improve biocompatibility, produce desirable pharmacokinetics, and promote effective intracellular trafficking.

To date, numerous materials have been evaluated as coatings for magnetic nanovectors including polymers, lipids, and peptides.[6, 7] Among these materials, cationic polymers, such as polyethylenimine (PEI) derivatized coatings, have been most commonly studied for construction of magnetic nanovectors.[7–14] PEI derivatized coatings are desirable because they endow a net cationic character to nanovectors at physiological pH that can be exploited for electrostatic adsorption of negatively charged nucleic acids. Additionally, the positive charge of the PEI coating facilitates intracellular delivery of nanovectors through adsorptive mediated endocytosis.[7] After cellular internalization, nanovectors must escape endosomal vesicles for proper intracellular trafficking to their site of action (e.g., nucleus for DNA, perinuclear region for siRNA). PEI can facilitate endosomal escape via the “proton sponge effect” wherein the influx of protons and counter-ions into the endosome increase the osmotic pressure leading to swelling and rupture of endosomes and release of its contents.[15] While PEI derivatized magnetic nanovectors have proven to be effective in vitro, this success has not always translated directly in vivo because of safety concerns and poor in vivo pharmacokinetics.

One major challenge is that cationic nanovectors interact with negatively charged serum proteins and cell membranes which can elicit many deleterious responses including: opsonization of nanovectors, rapid clearance, erythrocyte aggregation, and damage to blood vessels and clearance organs.[6] To circumvent these limitations researchers have primarily focused on approaches to neutralize the surface charge of cationic nanovectors in an effort to improve their safety.[7, 10] For example, our group and others have shown that derivatization of PEI with polyethylene glycol (PEG) can reduce the cytotoxicity of PEI based nanovectors.[10, 16–18] Furthermore, alkylated PEI coated onto magnetic nanocrystals was shown to be both effective and tolerable in an siRNA delivering nanovector in vivo.[13] These studies indicate that derivatization of PEI to achieve a delicate balance of minimizing cationic charge without compromising gene delivery efficacy may improve its cytotoxicity. However, the long-term accumulation of non-biodegradable, synthetic polymers, such as PEI, is still a major concern. Furthermore, no in vivo studies have proved the systemic safety and clearance of PEI derivatized nanovectors, both critical for clinical use.

An alternative to PEI for coating magnetic nanovectors is the naturally occurring polypeptides of arginine (pArg).[7, 9] Magnetic nanovectors coated with pArg are alternatively trafficked through a transcellular membrane diffusion pathway, and are more potent in delivering siRNA to cancer cells in vitro compared to PEI coated nanovectors.[9] In this study, we aimed to investigate the safety and efficacy of NP-pArg-siRNA in comparison to NP-PEI-siRNA for in vivo use. We evaluated their dose response for intracellular delivery and subsequent gene silencing in a C6 glioblastoma cell line in vitro. We further evaluated both the in vitro and in vivo safety profile of each nanovector formulation by examining their respective cytotoxicity, hemocompatibility, clearance organ uptake, and systemic toxicity.

MATERIALS AND METHODS

Materials

All reagents were purchased from Sigma Aldrich (St. Louis, MO) unless otherwise specified. Cy5 and Thiol modified siRNA (5′Cy5-GCAAGCUGACCCUGAAGUUCUU3′–antisense, 5′ thiol-GAACUUCAGGGUCAGCUUGCUU3′–sense) designed to knockdown green fluorescent protein (GFP) was purchased from Integrated DNA Technologies, Inc (IDT, San Diego, CA)

NP-pArg-siRNA and NP-PEI-siRNA Synthesis

The nanovectors NP-pArg-siRNA and NP-PEI-siRNA were prepared as previously described.[9, 19] Briefly, amine terminated PEG-coated iron oxide nanoparticles (NPs) were modified with cationic polymers of pArg (MW 10,000) or PEI (MW 10,000) through the formation of a thioether bond between thiolated polymers and NPs activated with iodoacetyl groups. Thiol modified siRNA oligonucleotides were then conjugated onto the nanoparticles through non-labile covalent bonds.

Gel Retardation Assay

Successful attachment of siRNA to NPs was assessed using gel retardation assays. A 4% low melting point agarose gel was prepared with 0.05 mg/mL ethidium bromide. While maintaining a uniform concentration of siRNA, samples of NP:siRNA complexes were prepared at weight ratios of 0:1, 0.5:1, 1:1, 5:1, 10:1, and 20:1 (Fe mass of NP to siRNA mass in NP:siRNA complex). The molar concentration of NPs can be calculated from the Fe mass for each 10 nm nanoparticle crystal assuming a volume of 5.2×10^{-25} m^3 and a density of 5.2 kg/m^3 based on the Fe_3O_4 crystal structure.[20] Using this method, we calculated that at a ratio of 20:1 (Fe mass of NP to siRNA mass NP:siRNA) approximately 4.3 molecules of siRNA are bound to each Fe_3O_4 nanoparticle crystal. Electrophoresis was run at 100 V for 1.5 hrs. Images were acquired on a Gel Doc XR (Bio-Rad Laboratories, Hercules, CA) and quantitated using the Quantity One software package (Bio-Rad Laboratories, Hercules, CA).

Nanovector Size and Zeta Potential Characterization

Hydrodynamic sizes and zeta potentials of the nanoparticle formulations were analyzed as 100 μg/mL (Fe equivalent) suspensions in 20 mM HEPES buffer (NaCl-free) (pH 7.4) using a DTS Zetasizer Nano (Malvern Instruments, Worcestershire, UK).

Cell Culture and Transfection Experiments

Enhanced green fluorescent protein (EGFP) expressing C6 rat glioma cells were produced as previously described.[8] Cells were maintained in Dulbecco's Modified Eagle Medium (DMEM, Invitrogen, Carlsbad, CA) supplemented with 10% FBS (Atlanta Biologicals, Lawrenceville, GA), 1 mg/mL G-418, and 1% antibiotic-antimycotic (Invitrogen, Carlsbad, CA) at 37°C and 5% CO_2.

Cell Transfection with Nanovectors

The day before transfection, cells were plated at 100,000 cells per well in 12-well plates. For transfection of cells with a nanovector formulation, cells were treated with the nanovector for 12 hrs under normal growth conditions. After the 12-hour incubation the media were replaced and cells incubated for an additional 48 hrs before analyses.

Cell Viability and Gene Silencing

Potential cytotoxicity was examined by the Alamar blue viability assay. After treatment, cells were washed thrice with PBS and incubated for 2 hrs with 10% Alamar blue (110 μg/mL resazurin) in DMEM (supplemented with 10% FBS and 1% antibiotic–antimycotic). The percent reduction of Alamar blue was determined following the manufacturer's protocol and used to calculate percent viability of treated samples (untreated cells represent 100% viability).

To quantify the degree of siRNA delivery and GFP gene silencing, treated cells were washed thrice with PBS and lysed with 1% Triton X-100 in PBS. Fluorescence from Cy labeled siRNA or GFP protein expression was measured using a SpectraMax microplate reader (Molecular Devices, Sunnyvale, CA). GFP fluorescence levels were normalized to the total number of viable cells, as determined by the Alamar blue viability assay. Relative GFP expression levels were then calculated based on the reduction in GFP expression as compared to non-transfected cells.

Transmission Electron Microscopy (TEM)

One million C6 cells were seeded in 25 cm^2 flasks 24 hrs before treatment. Cells were then treated with nanovector formulations as described for gene silencing experiments. Cells were then washed thrice with PBS and incubated with ice-cold Karnovsky's fixative for 24 hrs. Following fixation, cells were processed directly from flasks for sectioning. Cell sections were stained with osmium tetroxide, lead citrate, and uranyl acetate for TEM-contrast enhancement. Cell samples were then imaged with a Philips CM100 TEM at 100 kV with a Gatan 689 digital slow-scan camera.

Erythrocyte Aggregation and Lysis Assays

For the erythrocyte aggregation assay, whole blood (1 mL total) was collected from nude mice into tubes containing EDTA. Erythrocytes were pelleted through centrifugation at 1000× g and washed thrice with PBS before resuspending into 3 mL PBS. Nanovectors were mixed with erythrocytes in 400 μL PBS in 24-well plates to a final NP concentration of 100 μg/mL and a final 40-fold dilution of erythrocytes. Mixtures were incubated at 37°C for 1 hr before bright-field imaging.

For the erythrocyte lysis assay, whole blood was collected from nude mice into tubes containing heparin. Whole blood was mixed 1:1 with nanovectors for a final NP concentration of 100 μg/mL and incubated at 37°C for 45 min. PBS and 1% Triton X-100 were used as negative and positive controls, respectively. Erythrocytes were then pelleted by centrifugation at 1000× g and supernatants transferred to wells of a 96-well plate. Absorbance at 540 nm was measured on a SpectraMax microplate reader and normalized to samples without erythrocytes to correct for background NP absorbance. Percent hemolysis was calculated from the PBS subtracted NP absorbance divided by the PBS subtracted Triton X-100 absorbance.

Histopathological Evaluation and Hematology Assay

All mouse studies were conducted in accordance with University of Washington Institutional Animal Care and Use Committee (IACUC) approved protocols. Whole organs (liver, kidney, and spleen) of C57BL/6 mice were removed through necropsy and preserved in 10% formalin for 48 hrs. Tissues were then embedded in paraffin wax, sliced into 5 μm tick sections, and stained with hematoxylin and eosin (H&E) or Prussian blue/Nuclear Fast Red using standard clinical laboratory protocols. Microscopic images of tissues were acquired using an E600 upright microscope (Nikon) equipped with a CCD camera. Blood cell panels and serum aspartate aminotransferase (AST) and alanine aminotransferase (ALT)

levels were quantified 48 hours after intravenous administration of NP-PEI-siRNA (n = 5), NP-pArg-siRNA (n = 5), and mice receiving PBS injections (n = 5), and compared to the normal ranges reported in the literature. Three hundred microliters of blood was drawn from each mouse through cardiac puncture bleeds. Samples were then submitted to a veterinary pathology laboratory (Phoenix Laboratories, Everett, WA) for analysis.

RESULTS AND DISCUSSION

Nanovector Development

SPIONs (10–12 nm core diameter as determined by TEM) coated with amine terminated polyethylene glycol (PEG)[19] were derivatized with pArg or PEI cationic polymer and siRNA oligonucleotides to produce NP-pArg-siRNA and NP-PEI-siRNA.[9] The chemical scheme of NP-pArg-siRNA and NP-PEI-siRNA is shown in Figure 1. Each magnetic nanovector consists of a SPION core that is progressively layered with siloxane, PEG, and cationic polymer and siRNA (Figure 1a and b). The produced magnetic nanovectors were chemically compiled through covalent linkages consisting of siloxane bonds adhering PEG to NP cores, and thioether bonds adhering the cationic polymer and siRNA to the PEG layer (Figure 1c). The successful conjugation of each chemical constituent of the NP-pArg and NP-PEI formulations was previously verified using ^{1}H NMR.[9]

Development of nanovector formulations for in vivo applications requires careful consideration of the physiological environment (e.g., high salinity, digestive enzymes, charged biomolecules, blood cells) and rational design of nanovectors to ensure stability under such environments.[21] In the conjugation scheme developed for this study, covalent, non-labile linkages were used to assemble the various chemical constituents of the nanovector (Figure 1). This approach was designed to ensure that the nanovector construct remained intact during blood circulation, nanoparticle cellular internalization, and intracellular trafficking. Covalent attachment of siRNA oligonucleotides to nanovectors using non-labile chemistries have previously been investigated and shown to not interfere with the functionality of siRNA in promoting RNAi.[22] To favor the non-labile thioether bond formation over electrostatic binding of the negatively charged siRNA with cationic NP, the reaction was performed in a high ionic strength, slightly basic buffer.

We used a gel retardation assay to assess siRNA loading onto the nanovectors. NP-PEI-siRNA and NP-pArg-siRNA were prepared at various ratios of NP to siRNA ranging from 0:1 to 20:1 (Fe mass of NP:siRNA mass). Without purification, the reaction products were loaded into agarose gels and unbound siRNA was separated from NP-bound siRNA through electrophoresis. Figure 2 provides the quantitative values obtained from the gel retardation assay evaluating siRNA attachment to NP-pArg (Figure 2a) and NP-PEI (Figure 2b). As shown, siRNA conjugation to NP-pArg reached near completion at a ratio of 20:1 (NP:siRNA). On the other hand, siRNA conjugation to NP-PEI reached completion at a comparatively lower ratio of 10:1 (NP:siRNA). This variation in conjugation efficiency can be attributed to the higher amino functional group density associated with PEI polymer structure as compared to pArg (43 Da mass per amine for PEI vs. 58 Da mass per amine for pArg). Therefore, PEI provided more reactive groups for covalent attachment of siRNA. To maintain consistency in siRNA content within the nanovector formulations, a ratio of 20:1 (NP:siRNA) was used for the preparation of nanovector formulations for subsequent experiments in this study.

The hydrodynamic size and zeta potential of nanoparticles can drastically influence their in vivo functionality, clearance, and overall safety.[6] The hydrodynamic size for each nanovector formulation was measured by dynamic light scattering (DLS) and shown in Figure 2c. Mean volume-based diameters were 21 nm for NP-pArg-siRNA and 22 nm for

NP-PEI-siRNA, reflecting the combined contribution from iron oxide cores, polymeric coating, and siRNA modification to the overall hydrodynamic size measured for each nanovector formulation. From these results it is evident that the conjugation scheme developed for this study does not significantly affect the overall size of the nanovector regardless of polycationic coating. Notably, the hydrodynamic size distributions for both nanovectors were favorable for in vivo navigation and evasion of rapid clearance by the reticuloendothelial system (5 nm < d < 200 nm).[23]

DLS was also used to evaluate the zeta potential of each nanovector formulation (Figure 2d). The average zeta potentials were +2.1 mV for NP-pArg-siRNA and +29.8 mV for NP-PEI-siRNA. The higher zeta potential of NP-PEI-siRNA is likely a result of the higher charge density of PEI as compared to pArg. The high cationic charge of NP-PEI-siRNA measured from our developed nanovector formulation is consistent with other PEI based nanovector formulations developed for in vivo applications and reported to be tolerable in animal studies.[11, 13, 24, 25] Thus, the NP-PEI-siRNA formulation developed for our studies is representative of PEI based nanovectors previously reported in the literature, and serves as a suitable control for comparative evaluation of PEI and pArg based coatings in nanovector development.

SiRNA Internalization and Gene Silencing

Both nanovector formulations were evaluated in vitro for siRNA delivery and gene silencing in a GFP expressing rat glioblastoma cell line C6/GFP+. The internalization of siRNA into C6/GFP+ cells by nanovectors was evaluated using fluorescently labeled siRNA (Figure 3a). C6/GFP+ cells were treated with NP-pArg-siRNA or NP-PEI-siRNA over a broad concentration range (6.25–50 μg of Fe/mL corresponding to 23–188 nM siRNA). The uptake profiles of both nanovector formulations were similar at low treatment doses of 6.25 and 12.5 μg of Fe/mL. However, at elevated doses, NP-pArg-siRNA significantly outperformed NP-PEI-siRNA, and was able to deliver an approximately 3-fold higher concentration of siRNA to C6/GFP+ cells at the highest evaluated dose. These results indicate that NP-pArg-siRNA formulation was more efficient as an siRNA internalizing nanovector and capable of facilitating higher doses of siRNA internalization by C6/GFP+ cells in comparison to the NP-PEI-siRNA formulation. This enhanced capability of NP-pArg-siRNA can be attributed to its ability to enter cells through an energy independent transcellular diffusion pathway while NP-PEI-siRNA was trafficked through an energy dependent endocytosis pathway.[9, 26]

We next evaluated the efficacy of each nanovector formulation to promote GFP gene silencing in C6/GFP+ cells (Figure 3b). NP-pArg-siRNA treatment was more effective than NP-PEI-siRNA in silencing GFP expression at all treatment doses evaluated. At the highest treatment dose of 50 μg of Fe/mL, NP-pArg-siRNA (188 nM siRNA) produced a 62% gene knockdown efficiency compared to 34% by NP-PEI-siRNA, which represents a 1.8-fold enhancement in gene silencing potency. The 1.8-fold increase in gene knockdown was lower than the 3-fold increase in siRNA uptake using NP-pArg-siRNA, which was likely caused by the difference in intracellular trafficking of NP-pArg-siRNA and NP-PEI-siRNA. Although NP-pArg-siRNA provided more internalization of siRNA, NP-PEI-siRNA was more efficient at delivering internalized siRNA to its site of action.

Nanovector Cytotoxicity

Potential cytotoxic effects of the developed nanovector formulations were evaluated using a combination of Alamar blue cell viability assays and TEM imaging of cellular ultrastructures (Figure 4). C6/GFP+ cells were treated with NP-pArg-siRNA or NP-PEI-siRNA at 50 μg of Fe/mL for 12 hours as described for cell transfection experiments. Forty-

eight hours post-nanovector treatment, cell viability was measured in comparison to an untreated control. C6/GFP+ cells treated with NP-pArg-siRNA were found to be significantly more viable than those treated by NP-PEI-siRNA (Figure 4a). To further elucidate the mechanism of the increased cytotoxicity associated with NP-PEI-siRNA treatment compared to NP-pArg-siRNA treatment, the ultrastructures of nanovector treated C6/GFP+ cells were examined by TEM. The cellular membrane structure of NP-pArg-siRNA treated cells appeared intact, while NP-PEI-siRNA treated cell showed severe damage in membranes (Figure 4b). Similarly, damage to the mitochondrial organelle structure could be seen in images from NP-PEI-siRNA treated C6/GFP+ cells as evident by the destruction of mitochondrial membrane organization (Figure 4c). No mitochondrial damage was evident in NP-pArg-siRNA treated cells.

The combined Alamar blue cell viability and TEM ultrastructure imaging experiments showed the high cytotoxicity of NP-PEI-siRNA treatment and revealed the mechanism of toxicity (cell membrane and mitochondria damage). Conversely, the NP-pArg-siRNA formulation did not induce any alterations to the cellular or mitochondrial membrane structures and only reduced cell viability by 28% in comparison to the significantly higher 74% reduction in cell viability induced by NP-PEI-siRNA treatments. Previous reports in the literature have alluded to a potential mechanism for cytotoxicity effects of PEI and described this mechanism to be related to high cationic nature of the molecule disrupting cellular and mitochondrial membrane integrities leading to cell necrosis and apoptosis;[27] however, there was no direct experimental evidence for this postulation. Our TEM imaging experimentally confirmed the induction of these effects through NP-PEI-siRNA treatment of C6/GFP+ cells. Notably, the lack of any damage to cell membrane integrity after treatment with NP-pArg-siRNA demonstrated the safety of this formulation and justified further in vivo evaluations.

Nanovector Hemocompatibility

A major concern in the development of nanovectors for clinical applications is hemocompatibility.[5] This is particularly crucial for cationic nanovectors because of the potential of the charge-charge interaction between cationic NPs and anionic erythrocyte membranes in the blood that can cause erythrocyte aggregation.[28] This can decrease the blood half-life of the nanovector and also increase the risk of hemolysis and embolism.[29, 30] NP-PEI-siRNA and NP-pArg-siRNA formulations were both evaluated using an erythrocyte aggregation assay (Figure 5). NP-pArg-siRNA showed similar results to the phosphate buffer saline (PBS) where no evidence of erythrocyte aggregation or lysis was observed. However, NP-PEI-siRNA samples showed significant erythrocyte aggregation and loss of erythrocyte structure, which likely indicates the presence of lysis. Quantitative evaluation of hemolysis further confirmed that NP-PEI treatment did significantly induce a 3-fold higher degree of hemolysis in comparison to treatment with NP-pArg formulations (Supplemental Figure 1). Therefore, the hemocompatibility of NP-pArg-siRNA was much greater than NP-PEI-siRNA.

In Vivo Nanovector Toxicity and Clearance Organ Uptake

A major barrier to the clinical application of nanovectors is the potential toxicity of developed nanomaterial formulations. We screened the toxicities and clearance routes of the developed nanovector formulations using wild-type mice. Healthy, wild-type animals were utilized for these assays to examine specific nanoparticle-induced toxicities while avoiding possible false malignancies due to tumor-burden. For these experiments C57BL/6 mice were injected with 200 μL of NP-pArg-siRNA or NP-PEI-siRNA (500 μg of Fe/mL) through the tail vein and sacrificed 48 hours post-injection. Vital clearance organs (liver, spleen, and

kidneys) and blood were harvested postmortem for hemological and histopathological evaluations.

Accumulation of NP-pArg-siRNA and NP-PEI-siRNA nanovectors in clearance organs was assayed through Prussian blue staining of sections of livers, kidneys, and spleens. Organs were fixed in 10% formalin, embedded in paraffin, sectioned, and stained with Prussian blue to monitor the presence of iron from the nanovectors (Figure 6). The clearance of both nanovector formulations appeared to be similar, with accumulations evident in liver and spleen, but not kidney. This profile is consistent with other nanoparticle formulations reported in the literature.[5–7, 31]

To evaluate the liver toxicity of the developed NP-pArg-siRNA and NP-PEI-siRNA formulations, blood from nanovector injected mice and from control mice receiving PBS injections were hematologically assayed. Aspartate aminotransferase (AST) and alanine aminotransferase (ALT) liver enzyme serum levels were measured to evaluate any evidence of hepatotoxicity (Table 1). Liver enzyme serum levels of mice treated with NP-pArg-siRNA showed no significant elevation in AST and ALT as compared to the PBS control mice. Furthermore, both AST and ALT levels were within the normal ranges expected for these animals (Table 1).[32, 33] Conversely, treatment with NP-PEI-siRNA produced significant elevation of both serum ALT and AST levels in comparison to the PBS treated group, and were above the normal range expected for these animals (Table 1).

Additionally, the white blood cell (WBC) counts of treated animal were assayed to evaluate evidence of bone marrow toxicity. WBC counts for both NP-pArg-siRNA and NP-PEI-siRNA were within normal ranges for healthy animals (Table 1).[34] Notably, evidence of hemolysis was present in blood harvested from all animals treated with NP-PEI-siRNA nanovectors but not in blood samples obtained from PBS or NP-pArg-siRNA treated mice, corroborating results from the erythrocyte aggregation and hemolysis in vitro assays. Combined, no appreciable hematological abnormalities were observed in NP-pArg-siRNA treated mice suggesting that these nanovectors were well tolerated at the dose evaluated in this study. Conversely, NP-PEI-siRNA treatments produced significant deleterious effects suggesting hepatotoxicity and hemolysis.

Finally, we performed histological analyses on the clearance organs (kidney, spleen, and liver) to examine any signs of acute toxicity. Organs were harvested from NP-pArg-siRNA, NP-PEI-siRNA, or PBS injected mice 48 hrs after receiving injections, fixed in 10% formalin, embedded in paraffin, sectioned, and stained with hematoxylin and eosin (H&E, Figure 7). No significant alterations of tissue structures were evident in liver, kidney, or spleen sections obtained from NP-pArg-siRNA treated animals as compared to PBS injected animals. However, liver sections from NP-PEI-siRNA injected animals showed widespread areas of hepatocyte cell death, and destruction of the vascular bed and sinusoidal structures, all signs of hepatotoxicity. Further, the spleen sections from mice injected with NP-PEI-siRNA showed infiltration of red pulp into the white pulp, which could be a secondary effect of erythrogenesis consistent with presence of hemolysis observed in blood samples collected from these animals (Table 1). Combined, these data show that the NP-pArg-siRNA nanovector formulation was biocompatible and safe. Conversely, the NP-PEI-siRNA formulation produced acute toxicity to clearance organs.

CONCLUSIONS

Development of safe and effective nanovectors for in vivo siRNA delivery is a major scientific and technological challenge that has hindered the clinical application of RNAi based therapeutics. In this work, we compared the safety and efficacy of two formulations of

magnetic nanovectors, namely NP-pArg-siRNA and NP-PEI-siRNA. We demonstrated that the uptake, efficacy, and in vivo toxicity were highly dependent on the polymer coating. The NP-pArg-siRNA nanovector formulation was demonstrated to be safer and more effective as a siRNA delivery vehicle as compared to NP-PEI-siRNA. Further, we demonstrated that PEI modified nanovectors produced significant deleterious effects in vivo including hemolysis, erythrocyte aggregation, and acute organ toxicity. Given the improvement in efficacy and safety produced through pArg modification of nanovectors, this polymer should be considered as an alternative to PEI in the development of future nanovector constructs for improved safety and efficacy.

Supplementary Material

Refer to Web version on PubMed Central for supplementary material.

Acknowledgments

This work is supported in part by NIH grants (R01CA134213 and R01EB006043). O.V., F.M.K., and C.F. acknowledge the support through an NCI training grant (T32CA138312). F.M.K. also acknowledges support from the American Brain Tumor Association Basic Research Fellowship in Honor of Susan Kramer. We acknowledge laboratory assistance of Ms. Surya Kotha, Mr. Joseph Ayesh, and Mr. Cassra Clark. We acknowledge the use of resources at the Center for Nanotechnology, Department of Immunology, and Department of Pathology at the University of Washington.

References

1. Davidson BL, McCray PB Jr. Current prospects for RNA interference-based therapies. Nat Rev Genet. 2011; 12:329–40. [PubMed: 21499294]
2. Petrocca F, Lieberman J. Promise and challenge of RNA interference-based therapy for cancer. J Clin Oncol. 2011; 29:747–54. [PubMed: 21079135]
3. Pecot CV, Calin GA, Coleman RL, Lopez-Berestein G, Sood AK. RNA interference in the clinic: challenges and future directions. Nat Rev Cancer. 2011; 11:59–67. [PubMed: 21160526]
4. Pan X, Thompson R, Meng X, Wu D, Xu L. Tumor-targeted RNA-interference: functional non-viral nanovectors. Am J Cancer Res. 2011; 1:25–42. [PubMed: 21572539]
5. Kievit FM, Zhang M. Cancer nanotheranostics: improving imaging and therapy by targeted delivery across biological barriers. Adv Mater. 2011; 23:H217–47. [PubMed: 21842473]
6. Veiseh O, Gunn JW, Zhang M. Design and fabrication of magnetic nanoparticles for targeted drug delivery and imaging. Adv Drug Deliv Rev. 2010; 62:284–304. [PubMed: 19909778]
7. Kievit FM, Zhang M. Surface engineering of iron oxide nanoparticles for targeted cancer therapy. Acc Chem Res. 2011; 44:853–62. [PubMed: 21528865]
8. Veiseh O, Kievit FM, Fang C, Mu N, Jana S, Leung MC, Mok H, Ellenbogen RG, Park JO, Zhang M. Chlorotoxin bound magnetic nanovector tailored for cancer cell targeting, imaging, and siRNA delivery. Biomaterials. 2010; 31:8032–42. [PubMed: 20673683]
9. Veiseh O, Kievit FM, Mok H, Ayesh J, Clark C, Fang C, Leung M, Arami H, Park JO, Zhang M. Cell transcytosing poly-arginine coated magnetic nanovector for safe and effective siRNA delivery. Biomaterials. 2011; 32:5717–25. [PubMed: 21570721]
10. Kievit FM, Veiseh O, Bhattarai N, Fang C, Gunn JW, Lee D, Ellenbogen RG, Olson JM, Zhang M. PEI-PEG-Chitosan Copolymer Coated Iron Oxide Nanoparticles for Safe Gene Delivery: synthesis, complexation, and transfection. Adv Funct Mater. 2009; 19:2244–2251. [PubMed: 20160995]
11. Kievit FM, Veiseh O, Fang C, Bhattarai N, Lee D, Ellenbogen RG, Zhang M. Chlorotoxin labeled magnetic nanovectors for targeted gene delivery to glioma. ACS Nano. 2010; 4:4587–94. [PubMed: 20731441]
12. Mok H, Veiseh O, Fang C, Kievit FM, Wang FY, Park JO, Zhang M. pH-Sensitive siRNA nanovector for targeted gene silencing and cytotoxic effect in cancer cells. Mol Pharm. 2010; 7:1930–9. [PubMed: 20722417]

13. Liu G, Xie J, Zhang F, Wang Z, Luo K, Zhu L, Quan Q, Niu G, Lee S, Ai H, Chen X. N-Alkyl-PEI-Functionalized Iron Oxide Nanoclusters for Efficient siRNA Delivery. Small. 2011; 7:2742–9. [PubMed: 21861295]

14. Lee JH, Lee K, Moon SH, Lee Y, Park TG, Cheon J. All-in-one target-cell-specific magnetic nanoparticles for simultaneous molecular imaging and siRNA delivery. Angew Chem Int Ed Engl. 2009; 48:4174–9. [PubMed: 19408274]

15. Godbey WT, Wu KK, Mikos AG. Poly(ethylenimine) and its role in gene delivery. J Control Release. 1999; 60:149–160. [PubMed: 10425321]

16. Ogris M, Walker G, Blessing T, Kircheis R, Wolschek M, Wagner E. Tumor-targeted gene therapy: strategies for the preparation of ligand-polyethylene glycol-polyethylenimine/DNA complexes. J Control Release. 2003; 91:173–81. [PubMed: 12932649]

17. Burke RS, Pun SH. Extracellular barriers to in Vivo PEI and PEGylated PEI polyplex-mediated gene delivery to the liver. Bioconjug Chem. 2008; 19:693–704. [PubMed: 18293906]

18. Veiseh O, Kievit FM, Gunn JW, Ratner BD, Zhang M. A ligand-mediated nanovector for targeted gene delivery and transfection in cancer cells. Biomaterials. 2009; 30:649–57. [PubMed: 18990439]

19. Fang C, Bhattarai N, Sun C, Zhang MQ. Functionalized Nanoparticles with Long-Term Stability in Biological Media. Small. 2009; 5:1637–1641. [PubMed: 19334014]

20. Veiseh O, Sun C, Gunn J, Kohler N, Gabikian P, Lee D, Bhattarai N, Ellenbogen R, Sze R, Hallahan A, Olson J, Zhang M. Optical and MRI multifunctional nanoprobe for targeting gliomas. Nano Lett. 2005; 5:1003–8. [PubMed: 15943433]

21. Authier F, Posner BI, Bergeron JJ. Endosomal proteolysis of internalized proteins. FEBS Lett. 1996; 389:55–60. [PubMed: 8682206]

22. Singh N, Agrawal A, Leung AK, Sharp PA, Bhatia SN. Effect of nanoparticle conjugation on gene silencing by RNA interference. J Am Chem Soc. 2010; 132:8241–3. [PubMed: 20518524]

23. Longmire M, Choyke PL, Kobayashi H. Clearance properties of nano-sized particles and molecules as imaging agents: considerations and caveats. Nanomedicine. 2008; 3:703–717. [PubMed: 18817471]

24. Zhou T, Jia X, Li H, Wang J, Zhang H, AY, Zhang Z. New tumor-targeted nanosized delivery carrier for oligonucleotides: characteristics in vitro and in vivo. Int J Nanomedicine. 2011; 6:1527–34. [PubMed: 21845042]

25. Goyal R, Tripathi SK, Tyagi S, Sharma A, Ram KR, Chowdhuri DK, Shukla Y, Kumar P, Gupta KC. Linear PEI nanoparticles: efficient pDNA/siRNA carriers in vitro and in vivo. Nanomedicine : nanotechnology, biology, and medicine. 2011

26. Herce HD, Garcia AE, Litt J, Kane RS, Martin P, Enrique N, Rebolledo A, Milesi V. Arginine-rich peptides destabilize the plasma membrane, consistent with a pore formation translocation mechanism of cell-penetrating peptides. Biophys J. 2009; 97:1917–25. [PubMed: 19804722]

27. Moghimi SM, Symonds P, Murray JC, Hunter AC, Debska G, Szewczyk A. A two-stage poly(ethylenimine)-mediated cytotoxicity: implications for gene transfer/therapy. Mol Ther. 2005; 11:990–5. [PubMed: 15922971]

28. Dobrovolskaia MA, Patri AK, Simak J, Hall JB, Semberova J, De Paoli Lacerda SH, McNeil SE. Nanoparticle size and surface charge determine effects of PAMAM dendrimers on human platelets in vitro. Mol Pharm. 2012; 9:382–93. [PubMed: 22026635]

29. Dobrovolskaia MA, Clogston JD, Neun BW, Hall JB, Patri AK, McNeil SE. Method for analysis of nanoparticle hemolytic properties in vitro. Nano Lett. 2008; 8:2180–7. [PubMed: 18605701]

30. Neun BW, Dobrovolskaia MA. Method for analysis of nanoparticle hemolytic properties in vitro. Methods Mol Biol. 2011; 697:215–24. [PubMed: 21116971]

31. Veiseh O, Kievit FM, Ellenbogen RG, Zhang M. Cancer cell invasion: treatment and monitoring opportunities in nanomedicine. Advanced drug delivery reviews. 2011; 63:582–96. [PubMed: 21295093]

32. Loeb, WF.; Das, SR.; Harbour, LS.; Turturro, A.; Bucci, TJ.; Clifford, CB. In Pathobiology of the aging mouse. In: Mohr, U.; Dungworth, DL.; Capen, CC.; Carlton, WW.; Sunderberg, JP.; Ward, JM., editors. Clinical Biochemistry. Vol. I. ILSI Press; Washington DC: 1996. p. 3-19.

33. Wolford ST, Schroer RA, Gohs FX, Gallo PP, Brodeck M, Falk HB, Ruhren R. REFERENCE RANGE DATABASE FOR SERUM CHEMISTRY AND HEMATOLOGY VALUES IN LABORATORY-ANIMALS. Journal of Toxicology and Environmental Health. 1986; 18:161–188. [PubMed: 3712484]

34. Jain, NC. Vetrinary Hematology. Lea & Febiger; Philadelphia: 1993.

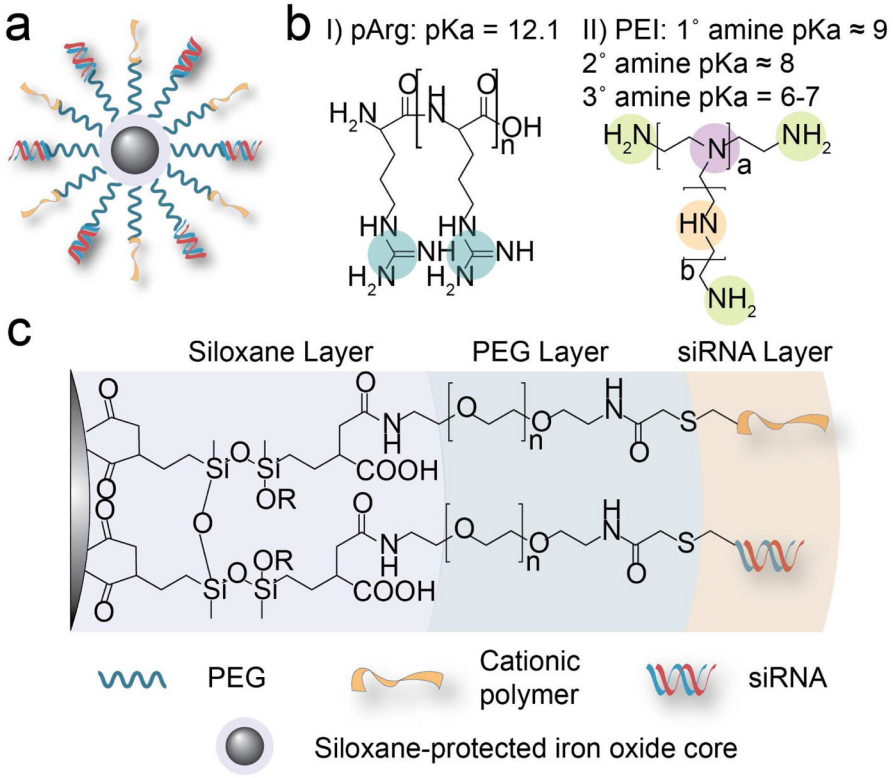

Figure 1.

Chemical structures of the magnetic nanovectors. (a) Magnetic nanovector architecture. (b) Chemical structures of the cationic polymers used to functionalize the NP to produce NP-pArg-siRNA and NP-PEI-siRNA. (c) Chemical composition of produced magnetic nanovectors.

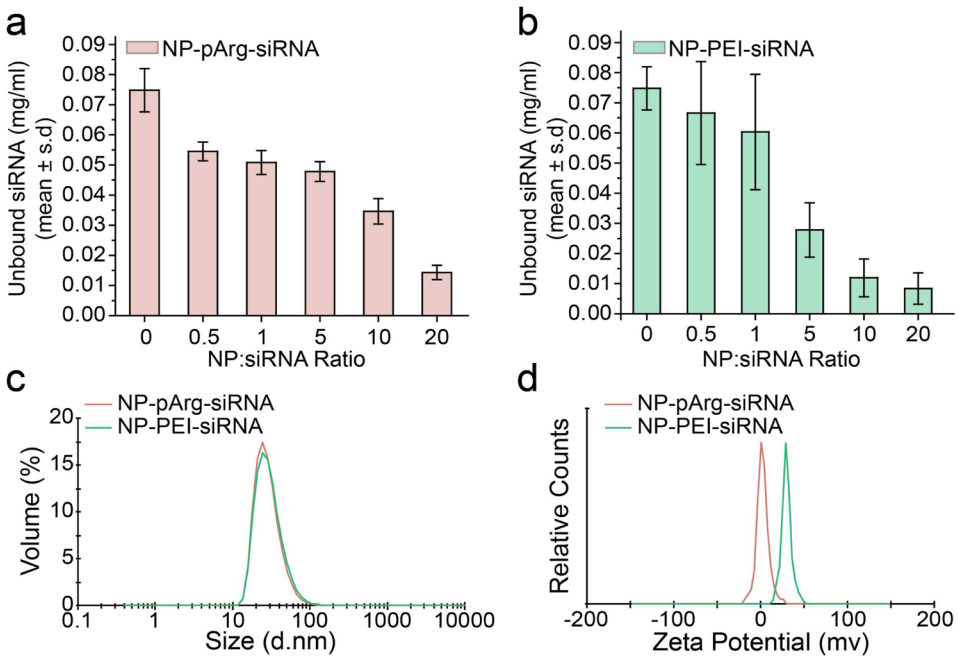

Figure 2.

Physicochemical characterizations of NP-pArg-siRNA, and NP-PEI-siRNA. Quantitative evaluation of the conjugation of siRNA onto (a) NP-pArg and (b) NP-PEI by a gel retardation assay. Ratios of NP to siRNA correspond to mass of NP (iron equivalent) to mass of siRNA. (c) Volume based hydrodynamic size distribution of NP-pArg-siRNA and NP-PEI-siRNA. (d) Zeta potentials of NP-pArg-siRNA and NP-PEI-siRNA.

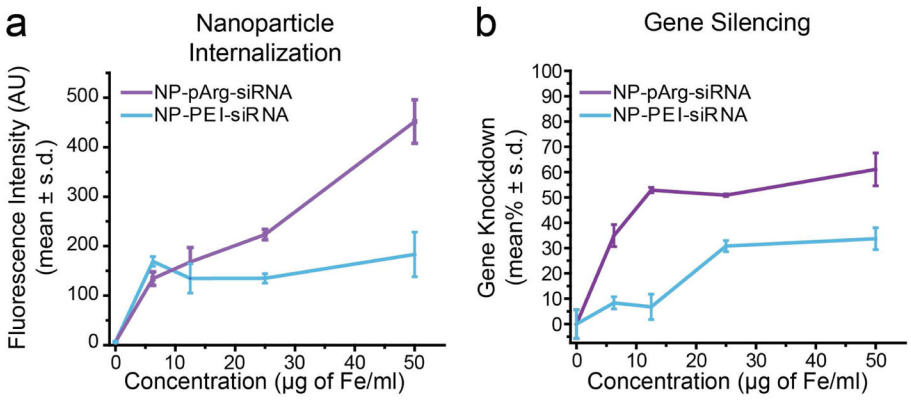

Figure 3.

In vitro dose-dependent nanovector internalization and GFP knockdown. (a) Uptake of nanovectors by target cells. (b) Efficiency of nanovector treatments on silencing GFP expression in C6/GFP+.

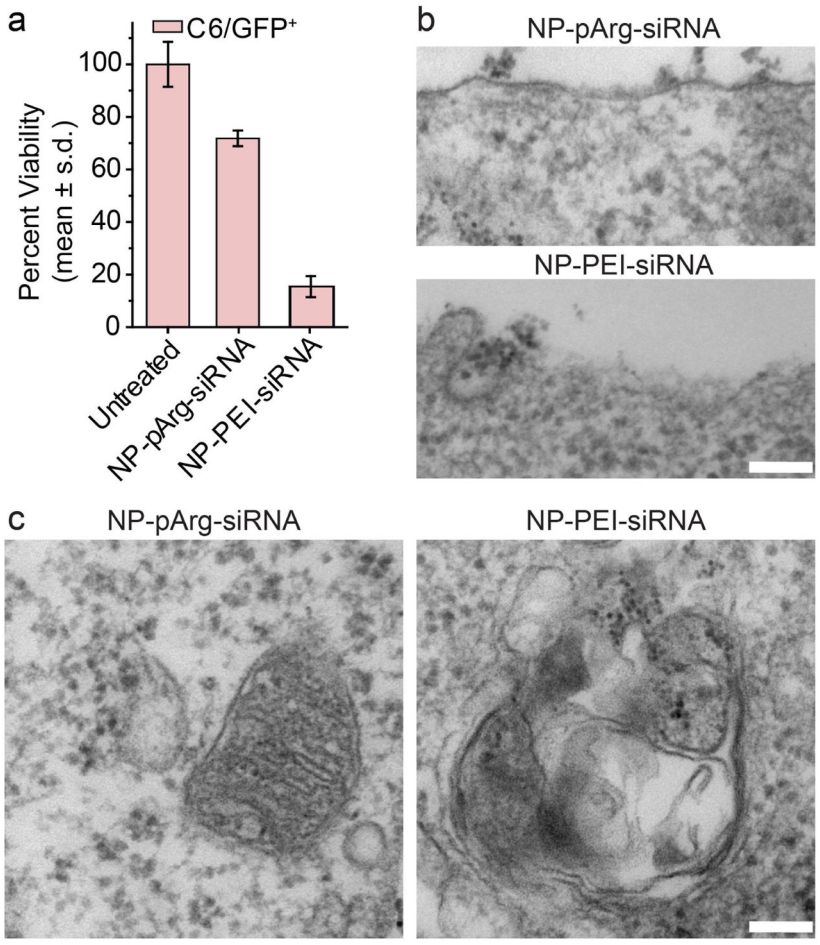

Figure 4.

Evaluation of nanovector toxicity. (a) Alamar blue cell viability assay (viability was normalized to untreated cells). TEM investigation of nanovector treatment effects on C6/GFP+ on plasma membrane structures (b), and mitochondrial membranes (c). The scale bars correspond to 100 nm.

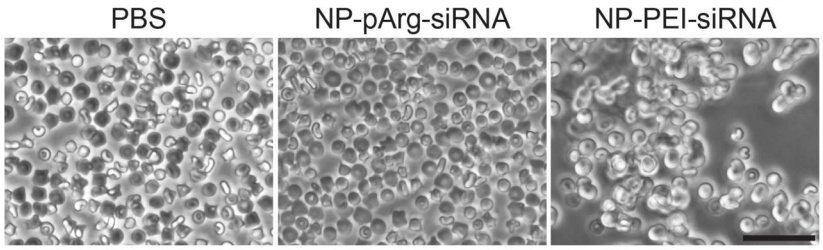

Figure 5.
Erythrocyte aggregation in the presence of PBS, NP-pArg-siRNA, or NP-PEI-siRNA nanovectors. The scale bar corresponds to 50 μm.

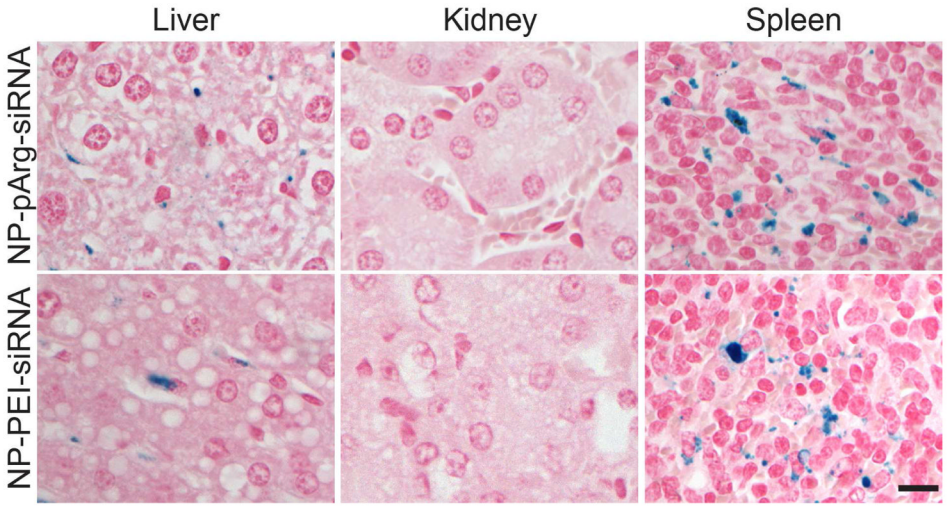

Figure 6.
Histological evaluation of nanovector clearance. Tissue sections from clearance organs (liver, kidney, and spleen) were collected from mice treated with NP-pArg-siRNA or NP-PEI-siRNA and stained with Prussian blue iron stain (blue) and nuclear fast red (pink). The scale bar corresponds to 50 μm.

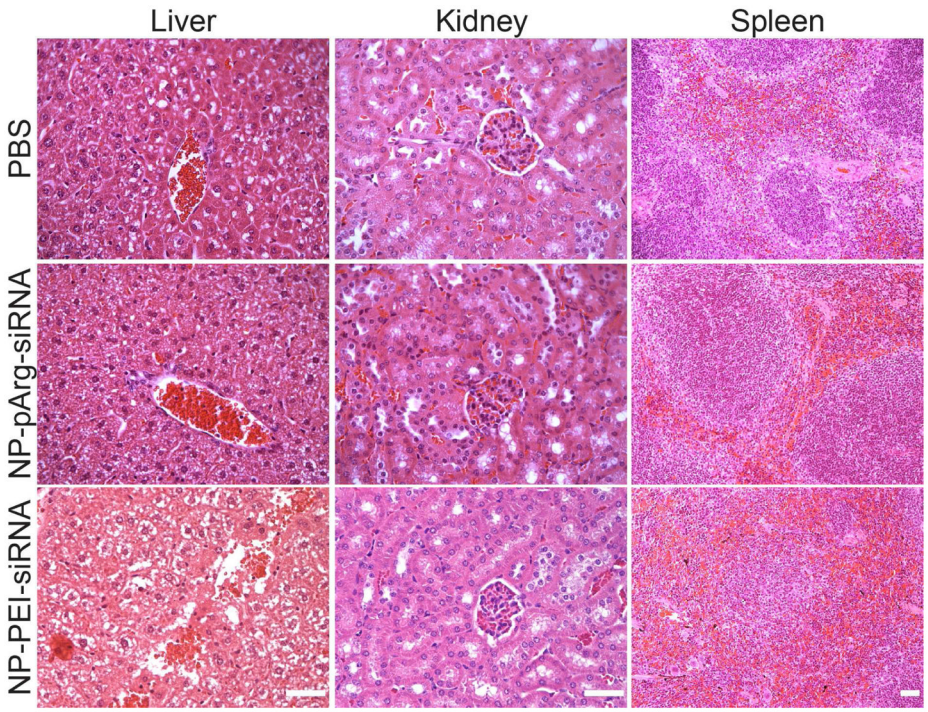

Figure 7.
H&E stained tissue sections of mouse liver, kidney, and spleen obtained from PBS, NP-pArg-siRNA, and NP-PEI-siRNA injected animals. The scale bars correspond to 50 μm.

Table 1

Live enzymalogy and hemocompatibility of nanovectors in mice treated with NP-pArg-siRNA, NP-PEI-siRNA, and PBS as a control.

Test	Units	PBS (mean ± s.d.)	NP-pArg- siRNA (mean ± s.d.)	NP-PEI-siRNA (mean ± s.d.)	Normal (mean range)
AST	U/L	200.0 ± 164.6	72.9 ± 11.1	2455 ± 222	49.6–171.2
ALT	U/L	38.3 ± 12.5	43.5 ± 12.0	591 ± 88	14.1–110.7
WBC	$\times 10^3/\mu L$	7.63 ± 2.63	4.56 ± 0.58	4.57 ± 0.32	3.56–10.29
Hemolysis	$+/-^a$	− − −	− − −	+ + +	

[a](+/−) indicate number of mice positive (+) or negative (−) for hemolysis.